Geometry and Physics of Catenanes Applied to the Study of DNA Replication

Ben Laurie,* Vsevolod Katritch,# Jose Sogo,§ Theo Koller,§ Jacques Dubochet,¶ and Andrzej Stasiak¶
*A. L. Digital, London W4 4GB, England; #Department of Chemistry, Rutgers University, New Brunswick, New Jersey 08903 USA; §Institut für Zellbiologie, ETH-Hönggerberg, CH-8093 Zürich, Switzerland; and ¶Laboratoire d'Analyse Ultrastructurale, Université de Lausanne, CH-1015 Lausanne-Dorigny, Switzerland

ABSTRACT The concept of ideal geometric configurations was recently applied to the classification and characterization of various knots. Different knots in their ideal form (i.e., the one requiring the shortest length of a constant-diameter tube to form a given knot) were shown to have an overall compactness proportional to the time-averaged compactness of thermally agitated knotted polymers forming corresponding knots. This was useful for predicting the relative speed of electrophoretic migration of different DNA knots. Here we characterize the ideal geometric configurations of catenanes (called *links* by mathematicians), i.e., closed curves in space that are topologically linked to each other. We demonstrate that the ideal configurations of different catenanes show interrelations very similar to those observed in the ideal configurations of knots. By analyzing literature data on electrophoretic separations of the torus-type of DNA catenanes with increasing complexity, we observed that their electrophoretic migration is roughly proportional to the overall compactness of ideal representations of the corresponding catenanes. This correlation does not apply, however, to electrophoretic migration of certain replication intermediates, believed up to now to represent the simplest torus-type catenanes. We propose, therefore, that freshly replicated circular DNA molecules, in addition to forming regular catenanes, may also form hemicatenanes.

INTRODUCTION

DNA catenanes are transient intermediates in such processes as replication of circular DNA or transposon resolution (Sundin and Varshavsky, 1980, 1981; Krasnow and Cozzarelli, 1983). By studying species of the formed catenanes, it is possible to get mechanistic insights into the termination process of DNA replication and into the mechanism of site-specific recombination (Sundin and Varshavsky, 1980; Spengler et al., 1985). To characterize the species of formed catenanes, it is necessary to separate different topological forms of DNA molecules by high-resolution agarose gel electrophoresis, so that the DNA isolated from different bands on gels could be analyzed by electron microscopy (Sundin and Varshavsky, 1980; Krasnow et al., 1983; Griffith and Nash, 1985). However, a high-quality electron microscope is not standard equipment in biochemical laboratories. Therefore, there is a need to find out the species of catenane just from its relative position on a gel containing some standard topological forms of DNA molecules with the same total length. Several theoretical (Lim et al., 1992; Lim and Janse van Rensburg, 1993) and experimental (Dean et al., 1985; Levene and Tsen, 1996) studies aimed to understand the gel separation of knotted DNA molecules. Already in the early 1980s, it was known that DNA catenanes or knots having the same molecular size increase their speed of electrophoretic migration with increasing number of nodes, i.e., the intersections of DNA segments in planar projections (Sundin and Varshavsky, 1980; Dean et al., 1985). However, these early gel systems did not succeed in separating different DNA knots with the same minimal crossing number, such as torus 5_1 and twist 5_2 knots (Dean et al., 1985). More recent works demonstrated, however, that in high-resolution agarose gels containing small amounts of SDS, torus-type of knots migrate more slowly than the twist-type of knots with the same minimal crossing number (Kanaar et al., 1990; Crisona et al., 1994). It was then observed that electrophoretic migration of identical size DNA molecules forming different knots is directly proportional to the overall compactness of ideal geometric configurations of the corresponding knots (Stasiak et al., 1996). Explanation for this electrophoretic behavior of knots was provided recently by establishing that the overall compactness of ideal forms of knots is directly proportional to the calculated sedimentation coefficient of thermally distorted knotted DNA molecules (Vologodskii et al., 1998). The sedimentation coefficient is a standard measure of molecular compactness, and as such is expected to determine the electrophoretic migration of corresponding types of DNA knots (Vologodskii et al., 1998). Here we investigate the correlation between the electrophoretic migration of different DNA catenanes and the overall compactness of ideal forms of the corresponding catenanes. Analyzing published gels, we observed that electrophoretic migration of torus-type catenanes of different complexities produced during site-specific recombination shows an approximately linear correlation with overall compactness of ideal forms of the corresponding catenanes. We were then very surprised when, among the intermediates of DNA

Received for publication 10 October 1997 and in final form 13 February 1998.

Address reprint requests to Dr. Andrzej Stasiak, Laboratoire d'Analyse Ultrastructurale, Bâtiment de Biologie, Université de Lausanne, CH-1015 Lausanne-Dorigny, Switzerland. Tel.: 41-21-6924282; Fax: 41-21-6924105; E-mail: andrzej.stasiak@lau.unil.ch.

0006-3495/98/06/2815/08 $2.00

replication believed to form a family of torus-type catenanes, one band failed to show this correlation. We argue here that the topological nature of this particular band was misinterpreted in the earlier studies. We propose that DNA molecules in this band form hemicatenanes, in which parental strands are still linked to each other, and two newly synthesized daughter strands are unlinked to each other.

METHODS

Simulations

Ideal configurations of catenanes were approached with computer simulations in which the entered initial configurations were randomly distorted, and the rules of Metropolis et al. (1953) were applied to search for the configuration that permitted maximization of the diameter of virtual cylinders centered on the axis of each component. The diameter was kept uniform and the same for both components of catenanes, but the axial length of both components could change independently. A new trial configuration was always accepted if it permitted an increase in the ratio of the diameter to the total length of both components ($d/l = f$), but when it led to a decrease in the ratio, the new trial configuration was accepted with a probability equal to $\exp((f_{new} - f_{old})a/RT)$. Here a is the normalization constant, R is the gas constant, and T is the temperature. Simulations were started at conditions corresponding to 800 K, and then, to stabilize the catenanes in their ideal form, a computational annealing was performed by simulating an exponential decrease in the temperature of the system toward 0 K.

Electron microscopy

Freshly replicated SV40 minichromosomes were cross-linked with psoralen, which resulted in interstrand DNA-DNA cross-links in a majority of nucleosomal linkers. Upon deproteinization, the DNA was spread under denaturing conditions and shadowed with platinum and carbon. A detailed experimental protocol is described by Sogo et al. (1986).

RESULTS

Ideal geometric forms of catenanes

The ideal geometric configuration of a knot or catenane is defined to be that which takes the least length of a tube with a uniform diameter to tie the given knot or catenane (Katritch et al., 1996). In practice, we use the ratio of the total length of the axial trajectory of both tubes forming a catenane to their uniform diameter as a scale-invariant measure. In our earlier work we used a computer simulation procedure to find ideal geometric configurations of different knots (Katritch et al., 1996). Here we modify our procedure to find the ideal configurations of different types of catenanes. Fig. 1 shows ideal geometric forms adopted by nine

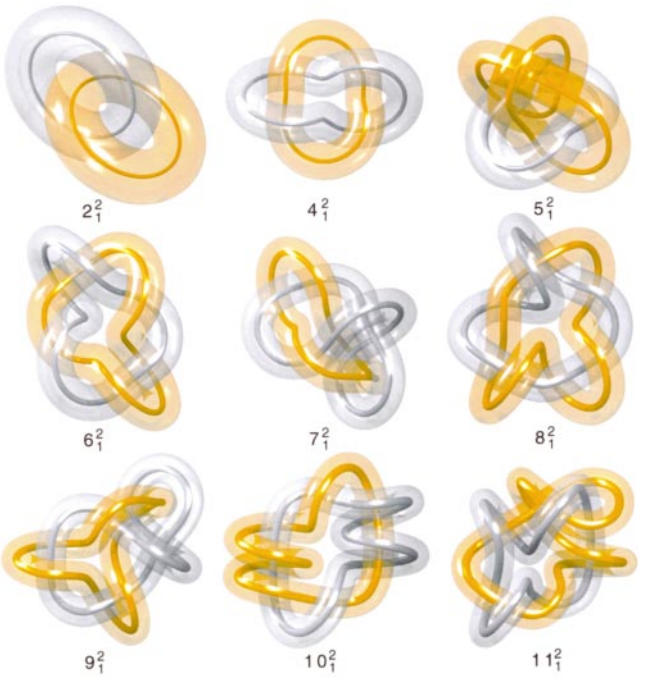

FIGURE 1 Ideal geometrical representations of various types of catenanes. Scale of the presentation of different catenanes is such that each occupies a similar space on the figure, whereby the length/diameter ratio grows from simpler to more complicated catenanes. The increasing thickness of the central nontransparent part indicates how much individual pictures were magnified from their original representation, where the total length of the two rings was equal for each presented type of catenane. Notice that, with the exception of the catenane 2_1^2, we cannot know whether the simulations really found the ideal geometric representations of the links, where the length/diameter ratio of the tube reaches its global minimum. The configurations presented are those that gave the smallest length/diameter ratio and were not improved upon in independent simulation runs.

different types of catenanes. The shown catenanes are composed of two closed tubes with uniform diameter. To facilitate visual tracing of both components of catenanes, we presented them as semitransparent tubes of different colors with nontransparent axial parts. In addition, upon generation of ideal configuration with a minimal length/diameter ratio, the diameter of the semitransparent tubes was shrunk by 10%, while the axial trajectory remained unchanged. The designations of catenanes follow the standard nomenclature in tables of knots and links, where the first number indicates a minimal crossing number in a planar projection for a given type of catenane, the superscript index number indicates the number of closed curves a given link is composed of, and the subscript index number indicates the tabular position of a given catenane among catenane types that have a given minimal number of crossings and are composed of a given number of closed curves (Rolfsen, 1976; Adams, 1994). During simulations the lengths of individual closed curves were allowed to vary, to permit the best distribution of the total length. So, for example, in the catenane 5_1^2 the longer, more contorted ring is approximately twice as longer as the other, almost planar ring. Notice that the sum of the length/diameter ratios of the tubes forming the ideal representa-

tions of catenanes increases with their increasing complexity. Table 1 presents the total length/diameter ratios of the ideal forms of different catenanes studied here (before 10% radial shrinking). Another characteristic property of ideal geometric representations of knots and catenanes is their average crossing number, which corresponds to the average number of crossings perceived when the axial trajectory of the ideal catenane is observed from all directions equisampling the sphere (see Table 1 for the corresponding values). Notice that for the presented ideal configurations of links (Fig. 1), the dominant pattern of winding of two components is such that locally one strand takes a central position and the second winds tightly around, and thus the pitch angle is minimized (this is easily visible in the catenane 10_1^2). This pattern was shown earlier to dominate in more complex, minimal-length torus knots in the cubic lattice (Janse van Rensburg, 1996).

While characterizing the ideal representations of knots, we noticed an approximately linear relationship between the length/diameter ratio and the average crossing number of different knots (Katritch et al., 1996). Thus we decided to check if a similar relation can also be observed for the links, although they are principally different from knots. In ideal links we optimize not only the trajectory of individual chains, but also the relative positions of the individual components. The average crossing number thus scores not only intrachain crossings, but also interchain crossings. Fig. 2 *A* shows that ideal forms of different catenanes show a quasilinear relationship between their length/diameter ratio and the average crossing number. It is interesting that at least for rather simple knots and links, it seems that this linear relationship can be described by a practically identical linear equation (see Fig. 2 *B*), and thus it is striking that with the increase in minimal length by two diameters, the average crossing number increases by approximately one. However, it must be stressed here that the perceived linearity between the length/diameter ratio and the average crossing number may be only a fair approximation for simple knots and links, whereas for more complex knots and links it was shown that this relation for different families of knots and catenanes will follow specific curves, where the average crossing number can grow more quickly than linearly with the increase in the *l*/*d* ratio of ideal knots and links (Cantarella et al., 1998; Buck, 1998).

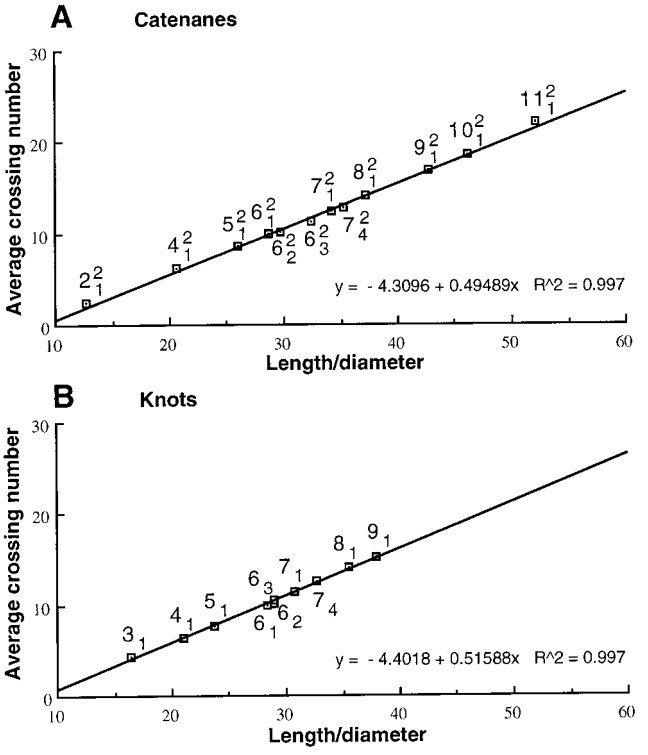

FIGURE 2 The linear relationship between the average crossing number and the length/diameter ratio in catenanes (*A*) and knots (*B*). Points corresponding to different types of catenanes and knots are marked accordingly. It is visible that the same linear equation approximates very well the relation between the average crossing number and the length/diameter ratio for catenanes and knots. Corresponding linear equations and the quality of fit are indicated.

TABLE 1 Characteristics of ideal geometrical representations of catenanes

Type of catenane	Length/diameter	Average crossing no.
2_1^2	12.7	2.4
4_1^2	20.6	6.2
5_1^2	26.0	8.6
6_1^2	28.7	9.9
6_2^2	29.7	10.1
6_3^2	32.3	11.2
7_1^2	34.1	12.4
7_4^2	35.2	12.8
8_1^2	37.2	14.0
9_1^2	42.7	16.8
10_1^2	46.1	18.6
11_1^2	52.1	22.1

The total length/diameter ratio was calculated directly for the ideal geometrical representation obtained in a computer simulation for a given type of catenane. To calculate the average crossing number, a modified Gaussian integral formula was used:

$$\frac{1}{4\pi}\sum_{i=1}^{j}\sum_{j=1}^{n}\oint_{C_i}\oint_{C_j}\left|\frac{(d\mathbf{r}_1\times d\mathbf{r}_2)\mathbf{r}_{12}}{\mathbf{r}_{12}^3}\right|.$$

On integration, the vectors $\mathbf{r}_1$ and $\mathbf{r}_2$ run over the contour *c*, corresponding to the axial trajectory of the ideal geometrical representation of a given catenane (Katritch et al., 1996).

Gel migration of DNA catenanes produced in site-specific recombination

Our earlier study revealed that the average crossing number in the ideal forms of different knots is directly proportional to the average crossing number in thermally agitated knotted polymers in solution forming the corresponding types of knots (Katritch et al., 1996). In addition, we showed recently that the average crossing numbers of different ideal knots are directly proportional to the sedimentation coefficient calculated for thermally agitated polymeric chains

(with a constant length) forming the corresponding knots (Vologodskii et al., 1998). Because the sedimentation coefficient is a standard measure of molecular compactness, it explains why the electrophoretic migration of different types of DNA knots (formed on the same size DNA molecules) showed a quasilinear correlation with the average crossing number of the ideal representation of the corresponding knot (Stasiak et al., 1996). To verify whether the ideal configurations of catenanes also "predict" time-averaged behavior of catenated DNA molecules in solution, we decided to check how the average crossing number of the ideal configurations of different catenanes correlate with the electrophoretic migration of corresponding types of DNA catenanes.

One of us participated in the earlier work, which determined what types of catenanes are produced in site-specific recombination reaction mediated by phage lambda integrase (Spengler et al., 1985). The analyzed catenanes all belonged to torus-type catenanes (2_1^2, 4_1^2, 6_1^2, 8_1^2, 10_1^2, etc.; see Fig. 1) and migrated during gel electrophoresis in specific bands; the higher the catenation number, the quicker was the migration of the band. Fig. 3 *A* shows how the distance of migration of different torus-type catenanes produced by lambda integrase correlates with the average crossing number of their ideal geometric configurations. It is apparent

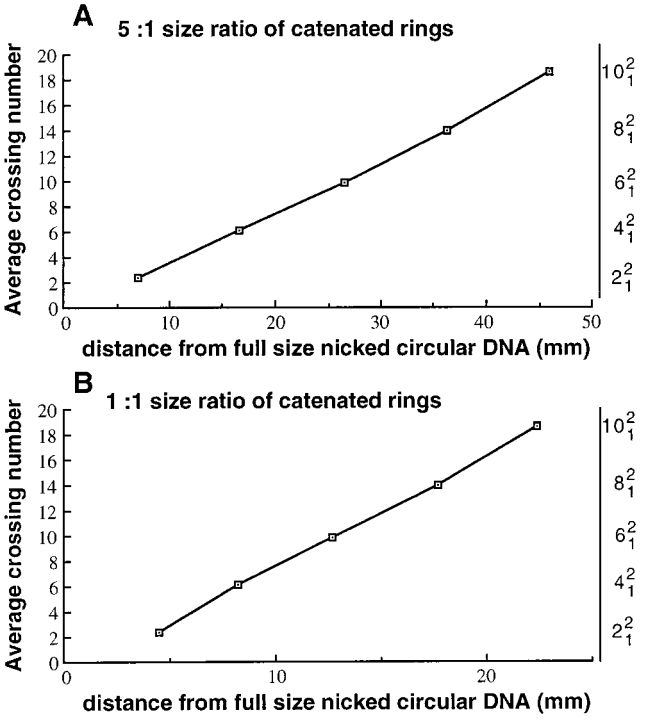

FIGURE 3 Linear correlation between electrophoretic migration of the torus type of catenanes and the average crossing number of corresponding ideal geometric configurations. (*A*) Torus type of catenanes, where one of the rings is about five times longer than the other. Electrophoretic migration was measured on the gel picture presented in figure 8 of Spengler et al. (1985). (*B*) Torus type of catenanes composed of two rings of nearly equal size. Electrophoretic migration was measured on the gel picture presented in figure 2 of Wasserman et al. (1988).

that the correlation is very good, despite the fact that analyzed DNA catenanes were composed of rings of unequal size, whereas in ideal configurations of these torus-type catenanes, the two rings reach the same size. This result indicates that the overall extent of the compactness in the catenanes composed of rings different in size is proportional to the extent of compactness in the catenanes with equal-sized rings. However, a more direct correlation should be expected between real and ideal catenanes composed of equal-sized rings. We thus turned to a more recent study of DNA catenanes produced in site-specific recombination, in which the formed torus-type catenanes (2_1^2, 4_1^2, 6_1^2, 8_1^2, 10_1^2, etc.) were composed of two rings of nearly equal size (Wasserman et al., 1988). These catenanes also formed a regularly spaced ladder of bands during electrophoresis, and their electrophoretic migration shows approximately linear correlation with the average crossing number of ideal configurations of these catenanes (Fig. 3 *B*). It probably goes without saying that DNA molecules migrating in the gel do not maintain the shape of the ideal configurations. However, as mentioned earlier, the overall dimensions of the thermally distorted configurations of different knots were shown to have a sedimentation coefficient (a standard measure of molecular compactness) directly proportional to the average crossing number of ideal configurations of the corresponding knots and links (Vologodskii et al., 1998). Because the gels discussed here are all run at low voltage in low-percentage agarose, the analyzed molecules tend to have a shape close to this at equilibrium in solution. Thus the average crossing number of ideal representations of knots and catenanes is still proportional to standard descriptors of molecular compactness, which as such seems to determine the speed of electrophoretic migration in low-percentage agarose gels. Therefore the more compact the equilibrium configuration, the smaller are the distortions needed to traverse the gel ,and thus the smaller the retardation during electrophoresis. However, it must be stressed here that in other gel systems (e.g., high voltage, denser matrix), properties of DNA molecules other than the sedimentation coefficient can be principal determinants of their electrophoretic migration.

Gel migration of DNA replication intermediates

In the early 1980s researchers studying the replication of circular DNA molecules noticed that just after finishing replication, the two daughter molecules frequently take on the form of torus catenanes (2_1^2, 4_1^2, 6_1^2, 8_1^2, 10_1^2, etc.; see Fig. 1) (Sundin and Varshavsky, 1980, 1981; Ullsperger et al., 1995). At that time, gel electrophoresis techniques were developed in which freshly replicated DNA molecules separated into a ladder of bands. The first band was believed to correspond to 2_1^2 catenanes, the second to 4_1^2, the third to 6_1^2, and so on (Sundin and Varshavsky, 1980). We used pictures of gels from these classical publications and from a more recent one (Adams et al., 1992) to compare how the migra-

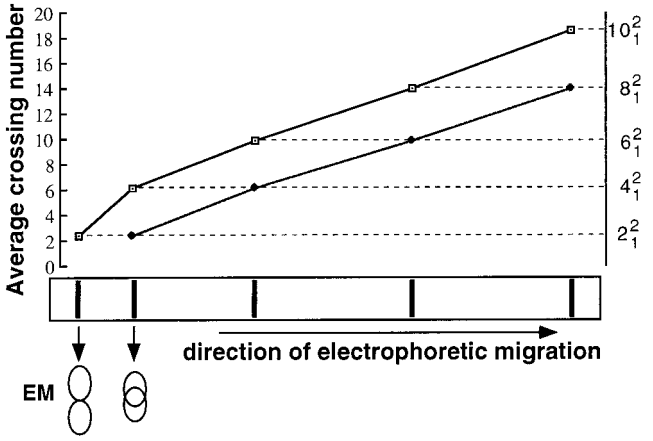

FIGURE 4 Two possible assignments of DNA bands on a gel containing replication products of circular SV40 viral DNA. The upper assignment was originally proposed by Sundin and Varshavsky (1980). However, in this assignment there is a poor linear fit between the electrophoretic migration and the average crossing number of different catenanes. A shift in the assignment allows for a much better linear relationship between the speed of electrophoretic migration and the average crossing number of ideal configurations of the corresponding catenanes. Data in this figure are based on figure 2 of Sundin and Varshavsky (1980), but also correspond to several other gels presented by Sundin and Varshavsky (1980, 1981). One can observe there that the expected regular spacing of bands containing torus type catenanes 2_1^2, 4_1^2, 6_1^2, etc. starts only from the second DNA band onward. (The same pattern is observed on gels analyzed by Adams et al. (1992).) This suggests to us that the first DNA band contains something other than 2_1^2 catenanes. Electron micrographs presented by Sundin and Varshavsky (1980) show, in fact, that DNA from the first band has the appearance of molecules with just one point of junction between the two DNA rings. Only in the material from the second band can one see molecules with two crossings, as expected for 2_1^2 catenanes (see figure 8, panel 6, in Sundin and Varshavsky, 1980).

tion of sequential bands of fresh replication products correlates with the length/diameter ratio of the ideal forms of torus-type catenanes. Because the catenanes formed during replication of circular DNA were believed to form exactly the same family as the catenanes analyzed by Wasserman et al. (1988), we expected a very similar, regularly spaced ladder of DNA bands, the more so because the gel systems were practically identical in studies by Sundin and Varshavsky (1980) and Wasserman et al. (1988). However, to our surprise, the first spacing between bands containing putative catenanes formed during DNA replication was less than half as wide as spacings between subsequent bands (Fig. 4). Looking for the reason for the discrepancy between the migration of DNA catenanes produced by site-specific recombination and the migration of replication intermediates, we returned to the paper that first established the DNA band assignment of DNA replication intermediates (Sundin and Varshavsky, 1980). This assignment was then copied in later papers analyzing fresh products of DNA replication (e.g., Adams et al., 1992). The original assignment was based on an analysis of electron micrographs of DNA species isolated from sequential bands on agarose gels (Sundin and Varshavsky, 1980). Reanalyzing these micrographs, we noticed that they were probably wrongly interpreted. Material from the first band did not have the appearance of a 2_1^2 catenane with the expected two crossings, but of two rings physically joined at a single point. Only the material from the second band contained some DNA molecules with the appearance of 2_1^2 catenanes. Upon correcting the assignment of the bands, we noticed very good agreement between the observed and predicted electrophoretic migration of DNA catenanes (Fig. 4).

However, another important question remains to be answered: What is the nature of the pointlike joining of freshly replicated molecules? Two possibilities should be considered: first, a recombination event leading to strand exchange between the two circular molecules and thus to formation of so-called figure 8 molecules (West et al., 1983; Colloms et al., 1997; Zerbib et al., 1997), and second, hemicatenation, in which only one strand of one double-stranded DNA molecule is catenated with one strand of the other double-stranded DNA molecule (Cunningham et al., 1981; Bianchi et al., 1983).

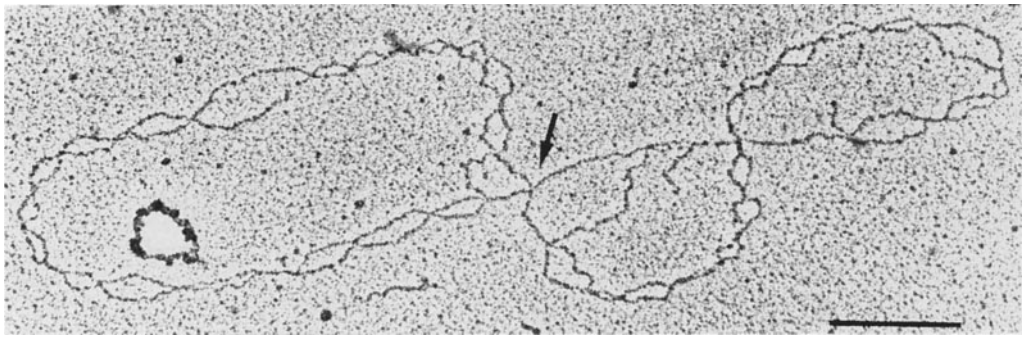

FIGURE 5 Electron micrograph of two joined but not freely catenated SV40 DNA molecules. The arrow points to the point of junction between two circular DNA molecules. The EM technique used allows for partial separation of the two DNA strands in each double-stranded circular DNA molecule. The presented picture is consistent with either a recombination intermediate stabilized by a point of strand exchange, or with a hemicatenane stabilized by the interlocking between two single strands. For more details about the material and EM procedure, see Sogo et al. (1986). The length of the magnification bar corresponds to 500 nucleotides of single-stranded DNA.

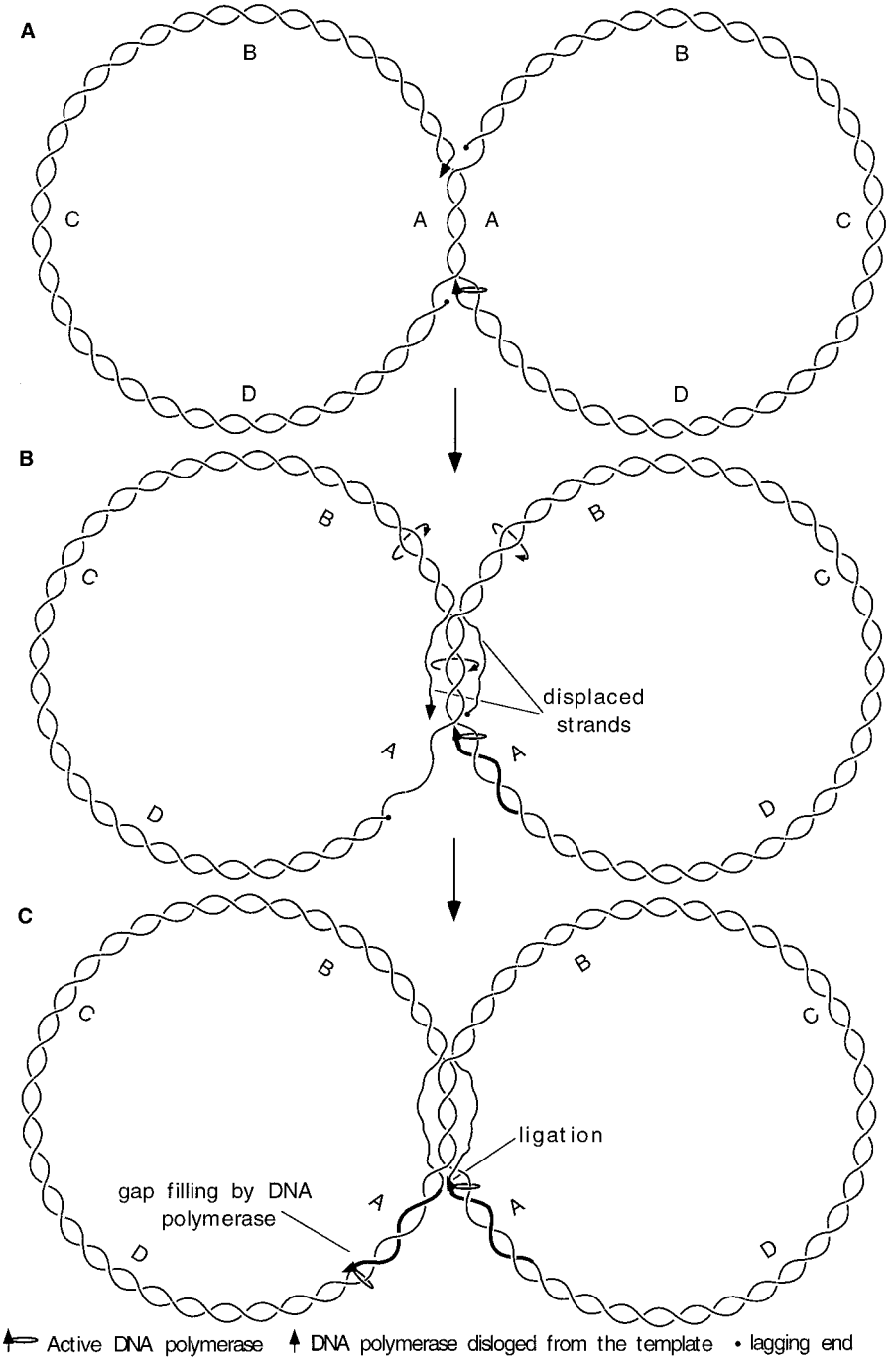

FIGURE 6 Termination of circular DNA replication via hemicatenation. (*A*) Cairns' structure with two remaining interlockings. In one of the forks, DNA polymerase becomes dislodged from the template. (*B*) Active DNA polymerase in the lower fork induces axial rotation and branch migration of the region of interlockings. This causes progressive displacement of leading and lagging strands from the other replication fork. A newly synthesized DNA strand is drawn with a thick line. Notice that the two interlocked molecules changed locations of the interlockings. (*C*) Upon reannealing of both displaced ends with the corresponding single-stranded regions exposed in the replication fork, the synthesis of both complementary strands can be terminated. The resulting hemicatenane is interlocked by the parental strands.

Hemicatenanes

In our earlier studies of replication of circular DNA molecules, we frequently observed replicated DNA molecules with point connections (Sogo et al., 1986). An electron micrograph of such a molecule spread under denaturing conditions upon psoralen cross-linking reveals a pointlike connection at the level of single-stranded DNA (Fig. 5). Similar pictures are presented in our earlier work (Sogo et al., 1986). Individual micrographs of such molecules do not allow us to conclude whether the two circular DNA molecules are joined by strand exchange or by a hemicatenation event. However, analysis of many pictures like the one in Fig. 5 revealed a lack of open Holliday junction configurations, which should be seen even more frequently than crossed configurations if a strand exchange process indeed took place between the two rings (Dressler and Potter, 1982). In addition, a homologous recombination event between identical DNA molecules should occur with equal frequency at every region, whereas the mapping of the junction region in psoralen cross-linked minichromosomes revealed that the junction was always at the region of the replication terminus (Sogo et al., 1986), which is consistent

with the formation of hemicatenanes during the final stages of DNA replication (see Fig. 6). Moreover, the fact that restriction endonuclease cleavage of one of the connected DNA rings in deproteinized molecules leads to their separation into linear and circular forms (Adams et al., 1992) is consistent with branch migration of hemicatenanes (Bianchi et al., 1983), but not with branch migration of classical Holliday junctions, which would produce α and σ structures only (West et al., 1983). These results therefore support an earlier suggestion that hemicatenanes are one of the intermediates of DNA replication (Sogo et al., 1986) (note that in the experiments described in the latter paper, the possibility of DNA branch migration was blocked by psoralen cross-linking). Fig. 6 schematically presents how hemicatenanes can be formed during replication of circular DNA by the process of branch migration induced by the advancing replication fork. According to the presented model in the late Cairns' structures, both replication forks try to make their way through the remaining few interlockings (Fig. 6 *A*). Advancing DNA polymerases displace DNA topoisomerases from the last region of nonreplicated DNA, and two ways of finishing replication are possible. In the first way (major pathway), leading end polymerases of the two forks advance toward each other, melting the remaining duplex region, and finish the replication by producing catenated DNA molecules (Sundin and Varshavsky, 1980, 1981). In the second, probably less frequent way (presented in Fig. 6), one of the advancing polymerases becomes dislodged from the template by the accumulated stress, so that only one fork advances. The advancing polymerase from the active fork "pushes" the interlocked region forward, and this induces a process of branch migration in which both the leading and lagging ends of DNA strands of the abandoned fork are progressively displaced (Fig. 6 *B*). When the displaced ends anneal back to complementary single-stranded regions of the advancing fork, the replication of both strands can be finished, and this results in hemicatenation (Fig. 6 *C*). Produced hemicatenanes can be later resolved by type I topoisomerase. However, the in vivo lifetime of the hemicatenanes can be long enough to permit their detection in a freshly replicated DNA isolated from cells containing active type I topoisomerase. Classical catenanes produced during terminal stages of DNA replication were observed upon isolation from cells containing active topoisomerase II, thus demonstrating that the in vivo lifetime of such intermediates is long enough for their transient accumulation (Sundin and Varshavsky, 1980). Data presented here support the proposed model (Fig. 6) of a new alternative pathway of DNA replication. Because the process of DNA replication is so vital, it is likely that several pathways exist to secure a correct termination of replication in the cases of different unfavorable situations.

We thank Prof. Piotr Pieranski for part of the data used in Fig. 2 *B*.

This work was supported by Swiss National Foundation grants 31-42158.94 and 31-41827.94, U.S. Public Health Service grant GM34809, the Foundation Herbette and A. L. Digital.

REFERENCES

Adams, C. C. 1994. The Knot Book. W. H. Freeman and Company, New York.

Adams, D. E., E. M. Shekhtman, E. L. Zechiedrich, M. B. Schmid, and N. R. Cozzarelli. 1992. The role of topoisomerase IV in partitioning bacterial replicons and the structure of catenated intermediates in DNA replication. *Cell.* 71:277–288.

Bianchi, M., C. DasGupta, and C. M. Radding. 1983. Synapsis and the formation of paranemic joints by *E. coli* RecA protein. *Cell.* 34: 931–939.

Buck, G. 1998. Four-thirds power law for knots and links. *Nature*. 392: 238–239.

Cantarella, J., R. B. Kusner, and J. M. Sullivan. 1998. Tight knot values deviate from linear relations. *Nature*. 392:237–238.

Colloms, S. D., J. Bath, and D. J. Sherrat. 1997. Topology of *Xer* mediated site-specific recombination at *psi* and *cer*. *Cell.* 88:855–864.

Crisona, N. J., R. Kanaar, T. N. Gonzalez, E. L. Zechiedrich, A. Klippel, and N. R. Cozzarelli. 1994. Processive recombination by wild-type Gin and an enhancer-independent mutant. Insight into the mechanisms of recombination selectivity and strand exchange. *J. Mol. Biol.* 243: 437–457.

Cunningham, R. P., A. M. Wu, T. Shibata, C. DasGupta, and C. M. Radding. 1981. Homologous pairing and topological linkage of DNA molecules by combined action of recA protein and topoisomerase I. *Cell.* 24:213–223.

Dean, F. B., A. Stasiak, T. Koller, and N. R. Cozzarelli. 1985. Duplex DNA knots produced by *Escherichia coli* topoisomerase I, structure and requirements for formation. *J. Biol. Chem.* 260:4975–4983.

Dressler, D., and H. Potter. 1982. Molecular mechanisms in genetic recombination. *Annu. Rev. Biochem.* 51:727–761.

Griffith, J. D., and H. A. Nash. 1985. Genetic rearrangement of DNA induces knots with a unique topology: implications for the mechanism of synapsis and crossing-over. *Proc. Natl. Acad. Sci. USA.* 82:3124–3128.

Janse van Rensburg, E. J. 1996. Lattice invariant for knots. *In* Mathematical Approaches to Biomolecular Structure and Dynamics. J. P. Mesirov, K. Shulten, and D. W. Sumners, editors. Springer Verlag, New York. 11–20.

Kanaar, R., A. Klippel, E. Shekhtman, J. M. Dungan, R. Kahmann, and N. R. Cozzarelli. 1990. Processive recombination by the phage Mu Gin system: implications for the mechanisms of DNA strand exchange, DNA site alignment and enhancer action. *Cell.* 62:353–366.

Katritch, V., J. Bednar, D. Michoud, R. G. Scharein, J. Dubochet, and A. Stasiak. 1996. Geometry and physics of knots. *Nature.* 384:142–145.

Krasnow, M. A., and N. R. Cozzarelli. 1983. Site-specific relaxation and recombination by Tn3 resolvase: recognition of the DNA path between oriented *res* sites. *Cell.* 32:1313–1324.

Krasnow, M. A., A. Stasiak, S. J. Spengler, F. Dean, T. Koller, and N. R. Cozzarelli. 1983. Determination of the absolute handedness of knots and catenanes of DNA. *Nature.* 304:559–560.

Levene, S. D., and H. Tsen. 1996. Analysis of DNA knots and catenanes by agarose-gel electrophoresis. *In* Protocols in DNA Topology and Topoisomerases, Vol. I. M. Bjornsti and N. Osheroff, editors. Humana Press, Clifton, NJ.

Lim, H. A., M. T. Carrol, and E. J. Janse van Rensburg. 1992. Electrophoresis of knotted DNA in a regular and a random electrophoretic medium. *In* Biomedical Modelling and Simulation. J. Eisenfield, D. S. Levine, and M. Witten, editors. Elsevier Science Publishers, New York. 213–223.

Lim, H. A., and E. J. Janse van Rensburg. 1993. A numerical study of the gel electrophoresis of knotted DNA. *Math. Model. Sci. Computing.* I:153–161.

Metropolis, N., A. W. Rosenbluth, M. N. Rosenbluth, A. H. Teller, and E. Teller. 1953. Equation of state calculations by fast computing machines. *J. Chem. Phys.* 21:1087–1092.

Rolfsen, D. 1976. Knots and Links. Publish or Perish Press, Berkeley, CA.

Sogo, J. M., H. Stahl, T. Koller, and R. Knippers. 1986. Structure of replicating simian virus 40 minichromosomes. The replication fork, core histone segregation and terminal structures. *J. Mol. Biol.* 189:189–204.

Spengler, S. J., A. Stasiak, and N. R. Cozzarelli. 1985. The stereostructure of knots and catenanes produced by phage λ integrative recombination: implications for mechanism and DNA structure. *Cell.* 42:325–334.

Stasiak, A., V. Katritch, J. Bednar, D. Michoud, and J. Dubochet. 1996. Electrophoretic mobility of DNA knots. *Nature.* 384:122.

Sundin, O., and A. Varshavsky. 1980. Terminal stages of SV40 DNA replication proceed via multiply intertwined catenated dimers. *Cell.* 21:103–114.

Sundin, O., and A. Varshavsky. 1981. Arrest of segregation leads to accumulation of highly intertwined catenated dimers: dissection of final stages of SV40 DNA replication. *Cell.* 25:659–669.

Ullsperger, C. J., A. V. Vologodskii, and N. R. Cozzarelli. 1995. Unlinking of DNA by topoisomerases during DNA replication. *Nucleic Acids Mol. Biol.* 9:115–142.

Vologodskii, A. V., N. Crisona, B. Laurie, P. Pieranski, V. Katritch, J. Dubochet, and A. Stasiak. 1998. Sedimentation and electrophoretic migration of DNA knots and catenanes. *J. Mol. Biol.* 278:1–3.

Wasserman, S. A., J. H. White, and N. R. Cozzarelli. 1988. The helical repeat of double-stranded DNA varies as a function of catenation and supercoiling. *Nature.* 334:448–450.

West, S. C., J. K. Countryman, and P. Howard-Flanders. 1983. Enzymatic formation of biparental figure-8 molecules from plasmid DNA and their resolution in *Escherichia coli. Cell.* 32:817–829.

Zerbib, D., S. D. Colloms, D. J. Sherrat, and S. C. West. 1997. Effect of DNA topology on Holliday junction resolution by *Escherichia coli* RuvC and bacteriophage T7 endonuclease I. *J. Mol. Biol.* 270:663–673.